

## TECHNICAL REPORT

# Three-dimensional cone-beam CT sialography in non tumour salivary pathologies: procedure and results

<sup>1</sup>Hélios Bertin, <sup>1</sup>Raphael Bonnet, <sup>2</sup>Anne-Sophie Delemazure, <sup>2</sup>Emmanuelle Mourrain-Langlois, <sup>1</sup>Jacques Mercier and <sup>1</sup>Pierre Corre

<sup>1</sup>Clinique de Chirurgie Maxillo-Faciale et Stomatologie, CHU de Nantes, Nantes, France; <sup>2</sup>Service d'Imagerie Médicale, CHU de Nantes, Nantes, France

**Objectives:** Non-tumour salivary diseases are common. Imaging studies are essential for their diagnosis and before undergoing an endoscopic or surgical treatment. In this study, we aimed at presenting our procedure and results obtained with three-dimensional CBCT (3D-CBCT) sialography for non-tumour salivary gland diseases.

**Methods:** Patients with parotid or submandibular salivary symptoms were examined by 3D-CBCT sialography. They received an intraductal injection of 0.5 mL of water-soluble contrast medium maintained in the gland, followed by examination in a NewTom wide-field CBCT device. Images were processed with multiplanar and 3D reconstructions.

**Results:** A ductal exploration could be performed until the fourth divisions. The main lesions found were stones, stenosis, dilatations and “dead tree” appearance of the ductal system. No side effects of the catheterization or the iodine contrast were reported, nor tissue damages related to the contrast keeping technique.

**Conclusions:** 3D-CBCT sialography seems to represent a reliable non-invasive diagnostic tool for ductal salivary diseases. More studies are needed to assess the value of 3D-CBCT sialography compared with conventional imaging.

*Dentomaxillofacial Radiology* (2017) **46**, 20150431. doi: 10.1259/dmfr.20150431

**Cite this article as:** Bertin H, Bonnet R, Delemazure A-S, Mourrain-Langlois E, Mercier J, Corre P. Three-dimensional cone-beam CT sialography in non tumour salivary pathologies: procedure and results. *Dentomaxillofac Radiol* 2017; **46**: 20150431.

**Keywords:** CBCT; sialography; salivary gland disease; diagnostic imaging

## Introduction

Non-tumour salivary gland diseases are common in adults and include sialadenitis, sialadenosis, stones, ductal strictures, dilatation and anatomical abnormalities.

Before undergoing endoscopic or surgical treatment, patients require radiological diagnosis and an accurate map of the salivary ducts to be generated.<sup>1,2</sup> A significant number of imaging procedures exist to explore the salivary ductal system, but no consensus on their use is available:

(1) Ultrasonography is a non-ionizing and inexpensive first-line examination allowing the diagnosis of tumours, salivary gland stones, collections and

abscesses. However, it is an operator-dependent imaging and may be inaccurate in detecting stones smaller than 2 mm.<sup>3,4</sup>

(2) Conventional sialography is the gold standard for diagnosing non-tumour salivary diseases,<sup>1,2,5</sup> allowing the ductal tree to be explored with high spatial resolution. Late evacuation shots provide information about the functionality of the gland. Sialography is advocated prior to any salivary gland endoscopy to calculate the diameter and degree of expansion of the excretory canal.

(3) MR sialography tends to replace conventional sialography.<sup>3</sup> Since MRI is non-ionizing and does not require cannulation, it can be used for the diagnosis of parenchymal and ductal lesions with

Correspondence to: Mr Hélios Bertin. E-mail: [helios.bertin@hotmail.fr](mailto:helios.bertin@hotmail.fr)

Received 21 December 2015; revised 9 August 2016; accepted 1 September 2016

simultaneous exploration of all the salivary glands.<sup>3,6</sup> Some disadvantages of MR include poor accessibility, high cost and a lower sensitivity when exploring ductal pathologies, since its resolution does not exceed the secondary divisions.<sup>5-7</sup>

- (4) Millimetre-thin axial CT scan slices, with multiplanar reconstruction (MPR) and three-dimensional (3D) reconstruction, are used to specify the number, size and location of salivary stones.<sup>8</sup> These offer higher specificity than ultrasonography and X-rays for stone disease.<sup>4</sup> With respect to the as low as reasonably achievable principle of radioprotection, CBCT has been proposed as an alternative to the CT scan.

3D-CBCT sialography was first described by Drage and Brown<sup>9</sup> in two patients with salivary gland obstruction previously explored with conventional sialography. To our knowledge, only 7 studies have been published, reporting 80 patients investigated with 3D-CBCT sialography.<sup>9-15</sup> A recent comparative study between two-dimensional plain radiograph and 3D-CBCT sialography in 47 patients demonstrated a better visualization of gland parenchyma, strictures and identification of sialoliths when using 3D-CBCT sialography.<sup>12</sup> The achievement procedure is most often underdescribed regarding the patient preparation.

In the light of poor literature, we aimed at presenting our full procedure and results obtained with 3D-CBCT sialography in non-tumour salivary gland diseases.

## Methods and materials

27 patients with main salivary gland symptoms such as chronic pain, swelling or recurrent infections were given a complete clinical examination followed by 3D-CBCT sialography. The procedure was accomplished at a later stage when the acute episode had subsided. Only symptomatic glands were examined. Patients were informed about the cannulation, the radiation generated and the potential risks of the procedure (stone mobilization, infection, allergy to the iodine contrast medium) and they gave their oral consent. After locating the salivary duct ostium, 0.5 mL of high-concentration, water-soluble, iodinated contrast product (HEXABRIX 320<sup>®</sup>, 320 g l<sup>-1</sup>; Guerbet, France) was injected under usual aseptic conditions using a lachrymal cannula (25G Moria<sup>®</sup> L12 mm; MORIA Inc., Doylestown, PA) until the patient felt fullness of the gland. The contrast medium was immediately maintained in the gland by placing a microsurgical clamp (Biover<sup>®</sup> TKM2, Hergiswil, Switzerland) on the ostium of the Wharton's duct (Figure 1) or with a plastic straight Halstead clamp placed on the ostium of the Stensen's duct. Local anaesthetic was given systematically near the ostium. Image acquisition was performed immediately after injection, in a seated patient, on a wide-field CBCT device (NewTom VGi, QR, Verona, Italy). Front and profile scout views were first achieved. Special exposure parameters were used to limit



**Figure 1** Microsurgical clamp placed on the ostium of the right Wharton's duct to maintain the contrast medium in the submandibular gland.

the radiation: reduced field of view 75 × 120 mm focused on the symptomatic gland, 110 kV, tube current and exposure time were modulated according to the scout views. The data acquisition time was 9 s.

Imaging data were archived in a picture archiving communication system (CARESTREAM<sup>®</sup> View PACS v. 11.3; Carestream Health, Inc., Rochester, NY, 2011). Analysis was performed on an imaging diagnosis workstation using maximal intensity projection, MPR with 0.3-mm cuts and 3D rendering. The entire ductal tree was explored focusing on the quantification and direct measurement of the lesions.

The radiation dose and early adverse effects of cannulation (bleeding, pain, canal perforation and iodine allergy) were systematically recorded.

## Results

3D-CBCT sialography allowed a precise 3D analysis of the ductal system until at least the fourth divisions,

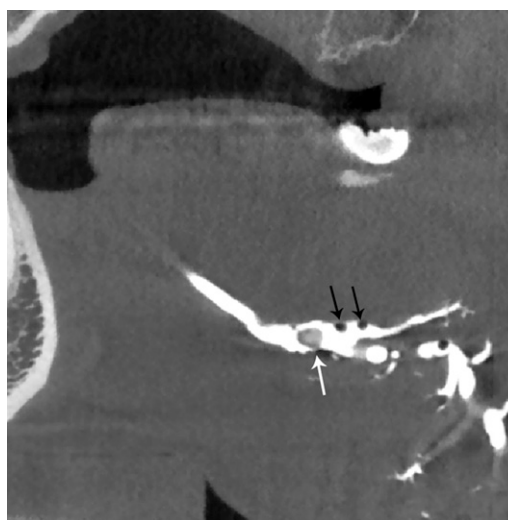


**Figure 2** Sagittal multiplanar reconstruction of the main duct of the right submandibular gland: a ductal-filling defect corresponding to a non-obstructive 3-mm stone of the hilum of the gland (white arrow). It can be noted that the air bubble images are appearing as multiple air defects (black arrows).

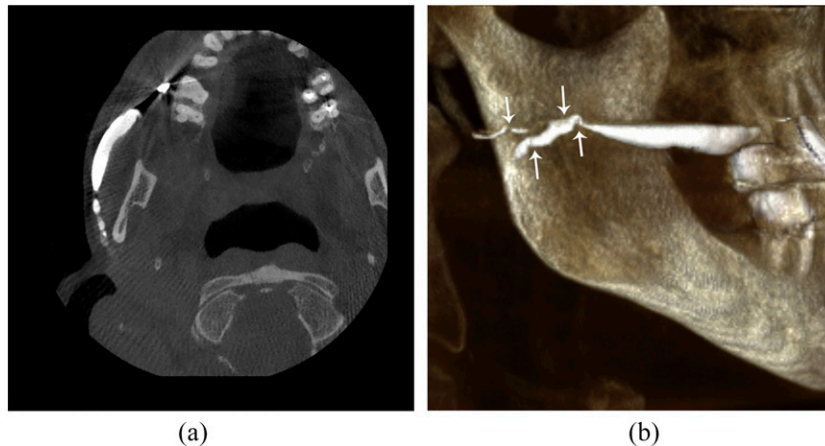


**Figure 3** Right Stensen's megaduct associated with bead-like strictures (arrows) in the distal third of the main duct without upstream opacification: (a) axial plan of the right parotid ductal system in multiplanar reconstruction. (b) Sagittal view of the ductal system of the right parotid gland in three-dimensional reconstruction.

regardless of the gland explored. The main lesions found were lithiasis and mucous plugs in 8 (29.6%) patients, evidenced by a ductal-filling defect (Figure 2) varying in density, shape and in fitting against the ductal wall. Stenosis of the primary, secondary or tertiary ducts were observed in eight cases (Figure 3). Chronic salivary injuries presenting as multiple ductal dilatations or distal "dead tree" appearance<sup>10</sup> were seen in 7 (25.9%) patients (Figure 4). Physiological anatomical plication of the Wharton's duct due to the duct looping over the lingual nerve<sup>16</sup> was assessed in two cases with the procedure (Figure 5). The main 3D-CBCT sialography findings are listed in table 1.

An average of 20 min (10–30 min) was required to prepare patients for 3D-CBCT sialography, depending on the difficulty in locating precisely the salivary duct ostium and the number of glands to investigate.

In our experience, of the 27 procedures achieved, we noted a 15% rate of failure, all in submandibular imaging. Artefacts of metal and dental origin did not interfere with image reading. No adverse effects were reported during catheterization or injection of the iodine contrast medium. Furthermore, no damage to the tissues related to the contrast-keeping technique was noted. The mean dose-area product generated by 3D-CBCT sialography was 552 mGy cm<sup>2</sup>, regardless of the gland studied.

### Discussion

The major salivary glands can be explored using ultrasonography, CT, MRI and sialography. Each of these radiological procedures have benefits and disadvantages.



**Figure 4** Inferior view of the main duct of the left submandibular gland in three-dimensional reconstruction: low tight stricture (arrow) in the distal third of the Wharton's duct with a distal "dead tree" appearance.

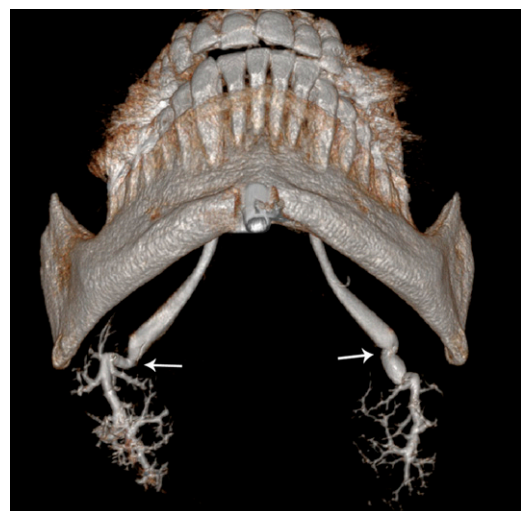


**Figure 5** Inferior view of the two submandibular ducts in three-dimensional reconstruction, showing bilateral anatomical kinking of the distal third of the Wharton's duct (arrows) with good upstream opacification.

**Table 1** Main three-dimensional CBCT (3D-CBCT) abnormality findings

<i>Ductal abnormalities</i>	<i>3D-CBCT findings</i>
Lithiasis	The sialolithiasis appears as hyperdense structure variable in shape (long, oval or round). The radiopaque contrast agent fills the duct proximally to the obstruction and usually flows around the lithiasis
Mucous plugs	Ductal-filling defect corresponding to a radiolucent sialolith
Stenosis	Single or multiple ductal stricture(s) mainly seen in the primary branching ducts. A good upstream opacification is obtained in case of permeable stenosis; no upstream opacification in tight strictures
Dilatations	Hilar and/or ductal enlargement often associated with obstruction. It can take the appearance of cavitory sialiectasis with contrast-filled peripheral cavities throughout the gland, seen in chronic sialadenitis and autoimmune disorders such as Sjögren syndrome
Dead tree appearance	Lack of contrast medium filling beyond the main duct and its primary branches corresponding to chronic salivary gland injuries
Anatomical plication of the Wharton's duct	Commonly observed proximal plication of the Wharton's duct due to the looping over of the lingual nerve after the duct exits the submandibular gland

With regard to literature analysis, 3D-CBCT sialography seems to be a powerful, safe and easily manageable examination to explore the major salivary glands. In this study, we aimed to assess the contribution of 3D-CBCT sialography to non-tumour salivary gland diseases and the modalities of its use.

3D-CBCT sialography allowed us to demonstrate the presence of stones mucous plugs, strictures and dilatations and to explore the normal glands. As with CT scanning or CBCT, 3D-CBCT sialography can determine the number and the precise location of salivary stones, including those smaller than 2 mm in diameter. The main advantage of this technique is that it allows accurate mapping of salivary ducts and injuries *via* 3D reconstruction and MPR. 3D-CBCT sialography is suitable for establishing an indication and guide a therapeutic endoscopic procedure.<sup>15</sup> Moreover, we think that cannulation of the salivary glands for radiological uses remains essential to our understanding of sialoendoscopy. We present a technique of contrast agent keeping in the gland, which allows better opacification of the whole ductal system and prevents contrast backflow. Reflux of contrast medium in the floor of the mouth has been described<sup>9</sup> and may interfere with image reading, particularly in the anterior lesions of the Wharton's duct. As previously outlined by Varoquaux

*et al*,<sup>10</sup> the image resolution is not altered by the presence of dental crowns, nor by metal clamps left in the mouth. Given that metal dental artefacts may invalidate CT scan and some MR pictures, this is clearly a major benefit of the 3D-CBCT technique.

In the absence of late evacuation shots, the functionality of the gland cannot be explored with the CBCT procedure. In addition, the gland parenchyma is not investigated. Our 15% failure rate with the procedure is within the limits found in the literature.<sup>7,17</sup> These failures were reported in submandibular imaging and linked to a difficulty of cannulation in three cases and an exclusive sublingual gland opacification without submandibular gland visualization in one case. Although cannulation performed during sialography exposes the patient to risk of infection, movement of the stone<sup>8</sup> and allergy to the contrast medium, we do not report any iatrogenic complications. The absence of tissue damage related to the contrast-keeping technique is probably owing to the use of non-traumatic microsurgical clamp usually employed in vascular surgery. The doses from CBCT are significantly lower than those of the CT scan but remain higher than those of conventional radiographs.<sup>18</sup> A recent study highlighted the possibility to obtain a similar effective dose between CBCT sialography and plain radiograph sialography,

**Table 2** Benefits and disadvantages of the three-dimensional CBCT (3D-CBCT) sialography

<i>Expected benefits of 3D-CBCT sialography</i>
Accurate mapping of salivary ducts and injuries
Number and precise location of salivary stones, including those inferior than 2 mm
Quick and easy access
Contrast medium keeping: better opacification of the ductal system, absence of contrast backflow interfering with image reading
Image reading not altered by dental crowns
<i>Disadvantages of the 3D-CBCT sialography</i>
No exploration of the functionality of the gland
No investigation of the gland parenchyma
Duct cannulation, pain, possible duct perforation
Achievable approximately 3–6 weeks after acute infective or inflammatory episode
Possible mobilization of stones, infection, allergy to the iodine contrast medium
Contrast medium keeping: damages to the surrounding tissues
Radiation generated



by using a reduced 15-cm field of view in combination with modulation of exposure parameters.<sup>19</sup> The theoretical benefits and disadvantages related to 3D-CBCT sialography are listed in [table 2](#).

In the present work, we described our modality of achievement of 3D-CBCT sialography and the benefits of keeping the contrast medium in the gland. We presented some results obtained with this new imaging tool. The main lack of this study is in the absence of comparison with other radiologic imaging tools. Recent works suggested that 3D-CBCT sialography outperformed conventional sialography and ultrasonography for the visualization of the intraglandular ductal system and identification of sialoliths.<sup>10,12,15</sup> Further large comparative studies are needed to assess the value of

3D-CBCT sialography for the diagnosis of non-tumour salivary diseases.

## Conclusions

In this technical note, we describe our technique of carrying out 3D-CBCT sialography and some results obtained with this imaging procedure. This examination combines the advantages of conventional sialography and CBCT to establish a salivary ductal map with a precise location of the lesions. More controlled studies are needed to determine the value of 3D-CBCT sialography in non-tumour salivary diseases.

## References

1. Iro H, Zenk J, Escudier MP, Nahlieli O, Capaccio P, Katz P, et al. Outcome of minimally invasive management of salivary calculi in 4,691 patients. *Laryngoscope* 2009; **119**: 263–8. doi: <https://doi.org/10.1002/lary.20008>
2. Katz P. New techniques for the treatment of salivary lithiasis: sialoendoscopy and extracorporeal lithotripsy: 1773 cases. [In French.] *Ann Otolaryngol Chir Cervicofac* 2004; **121**: 123–32.
3. Marchal F. Salivary gland endoscopy: new limits? [In French.] *Rev Stomatol Chir Maxillofac* 2005; **106**: 244–9.
4. Avrahami E, Englender M, Chen E, Shabtay D, Katz R, Harell M. CT of submandibular gland sialolithiasis. *Neuroradiology* 1996; **38**: 287–90. doi: <https://doi.org/10.1007/BF00596550>
5. Katz P. Imagerie normale des glandes salivaires. In: *EMC Radiodiagnostic—Coeur poumons*. Paris: Elsevier Masson SAS; 2006.
6. Tassart M, Zeitoun D, Ifenecker C, Bahlouli F, Bigot JM, Boudghène F. MR sialography. [In French.] *J Radiol* 2003; **84**: 15–26.
7. Kalinowski M, Heverhagen JT, Rehberg E, Klose KJ, Wagner HJ. Comparative study of MR sialography and digital subtraction sialography for benign salivary gland disorders. *AJNR Am J Neuroradiol* 2002; **23**: 1485–92.
8. Faye N, Tassart M, Périé S, Deux JF, Kadi N, Marsault C. Imaging of salivary lithiasis. [In French.] *J Radiol* 2006; **87**: 9–15.
9. Drage NA, Brown JE. Cone beam computed sialography of sialoliths. *Dentomaxillofac Radiol* 2009; **38**: 301–5. doi: <https://doi.org/10.1259/dmfr/90784441>
10. Varoquaux A, Larribe M, Chossegros C, Cassagneau P, Salles F, Moulin G. Cone beam 3D sialography: preliminary study. [In French.] *Rev Stomatol Chir Maxillofac* 2011; **112**: 293–9. doi: <https://doi.org/10.1016/j.stomax.2011.08.017>
11. Hunsaker RB, Cunningham L, Yepes JF. Combined CBCT and sialogram: report of three cases. *Gen Dent* 2012; **60**: e221–223.
12. Jadu FM, Lam EW. A comparative study of the diagnostic capabilities of 2D plain radiograph and 3D cone beam CT sialography. *Dentomaxillofac Radiol* 2013; **42**: 20110319. doi: <https://doi.org/10.1259/dmfr.20110319>
13. Abdel-Wahed N, Amer ME, Abo-Taleb NS. Assessment of the role of cone beam computed sialography in diagnosing salivary gland lesions. *Imaging Sci Dent* 2013; **43**: 17–23. doi: <https://doi.org/10.5624/isd.2013.43.1.17>
14. Shahidi S, Hamedani S. The feasibility of cone beam computed tomographic sialography in the diagnosis of space-occupying lesions: report of 3 cases. *Oral Surg Oral Med Oral Pathol Oral Radiol* 2014; **117**: e452–7. doi: <https://doi.org/10.1016/j.oooo.2014.02.023>
15. Kroll T, May A, Wittekindt C, Kähling C, Sharma SJ, Howaldt HP, et al. Cone beam computed tomography (CBCT) sialography—an adjunct to salivary gland ultrasonography in the evaluation of recurrent salivary gland swelling. *Oral Surg Oral Med Oral Pathol Oral Radiol* 2015; **120**: 771–5. doi: <https://doi.org/10.1016/j.oooo.2015.09.005>
16. Abubaker AO, Lam D, Benson KJ. *Oral and maxillofacial surgical secrets*: Elsevier Health Sciences; 2015. p. 557.
17. Jäger L, Menauer F, Holzknicht N, Scholz V, Grevers G, Reiser M. Sialolithiasis: MR sialography of the submandibular duct—an alternative to conventional sialography and US? *Radiology* 2000; **216**: 665–71.
18. Roberts JA, Drage NA, Davies J, Thomas DW. Effective dose from cone beam CT examinations in dentistry. *Br J Radiol* 2009; **82**: 35–40. doi: <https://doi.org/10.1259/bjr/31419627>
19. Jadu F, Yaffe MJ, Lam EW. A comparative study of the effective radiation doses from cone beam computed tomography and plain radiography for sialography. *Dentomaxillofac Radiol* 2010; **39**: 257–63. doi: <https://doi.org/10.1259/dmfr/62878962>